The EMBO Journal (2005) 24, 4415–4424 | © 2005 European Molecular Biology Organization | All Rights Reserved 0261-4189/05
www.embojournal.org

THE EMBO JOURNAL

Phosphorylation by casein kinase 2 induces PACS-1 binding of nephrocystin and targeting to cilia

Bernhard Schermer[1,5], Katja Höpker[1,5] Heymut Omran[2,5], Cristina Ghenoiu[1], Manfred Fliegauf[2], Andrea Fekete[2], Judit Horvath[2], Michael Köttgen[1], Matthias Hackl[1], Stefan Zschiedrich[1], Tobias B Huber[1], Albrecht Kramer-Zucker[1], Hanswalter Zentgraf[3], Andree Blaukat[4], Gerd Walz[1] and Thomas Benzing[1,*]

[1]Renal Division, University Hospital Freiburg, Freiburg, Germany, [2]Childrens Hospital, University Hospital Freiburg, Freiburg, Germany, [3]Deutsches Krebsforschungszentrum, Heidelberg, Germany and [4]Department of Pharmacology, University of Heidelberg, Heidelberg, Germany

Mutations in proteins localized to cilia and basal bodies have been implicated in a growing number of human diseases. Access of these proteins to the ciliary compartment requires targeting to the base of the cilia. However, the mechanisms involved in transport of cilia proteins to this transitional zone are elusive. Here we show that nephrocystin, a ciliary protein mutated in the most prevalent form of cystic kidney disease in childhood, is expressed in respiratory epithelial cells and accumulates at the base of cilia, overlapping with markers of the basal body area and the transition zone. Nephrocystin interacts with the phosphofurin acidic cluster sorting protein (PACS)-1. Casein kinase 2 (CK2)-mediated phosphorylation of three critical serine residues within a cluster of acidic amino acids in nephrocystin mediates PACS-1 binding, and is essential for colocalization of nephrocystin with PACS-1 at the base of cilia. Inhibition of CK2 activity abrogates this interaction and results in the loss of correct nephrocystin targeting. These data suggest that CK2-dependent transport processes represent a novel pathway of targeting proteins to the cilia.

The EMBO Journal (2005) **24,** 4415–4424. doi:10.1038/sj.emboj.7600885; Published online 24 November 2005
Subject Categories: molecular biology of disease
Keywords: cilia; cystic kidney disease; nephrocystin; NPHP1; PACS-1

Introduction

Cilia are highly conserved organelles that project from the surfaces of many cells (Igarashi and Somlo, 2002). The essential structure of cilia consists of nine peripheral microtubule doublets forming the axoneme, surrounded by a membrane lipid bilayer that is continuous with the plasma membrane. Based on whether the axoneme includes an additional central pair of microtubules, cilia are classified as '9 + 2' or '9 + 0' cilia (Rosenbaum and Witman, 2002; Hiesberger and Igarashi, 2005). Some cilia contain additional dynein arms and are motile (Ibanez-Tallon *et al*, 2003). The ciliary axoneme emerges from the basal body, a microtubule-based structure that also functions as the spindle-organizing center in mitosis. The boundary between the cellular and ciliary compartments is demarcated by an area called the transition zone (Rosenbaum and Witman, 2002; Snell *et al*, 2004). Mutations in proteins localized to cilia and basal bodies have been implicated in a growing number of genetic diseases, ranging from cystic kidney and retinal degenerative disease to respiratory and neurologic disorders, diabetes, and obesity (Calvet, 2002; Pazour and Rosenbaum, 2002; Ansley *et al*, 2003; Pan *et al*, 2005). Access of proteins to the ciliary compartment requires targeting to the base of the cilia, the basal body, and the transition zone. However, the mechanisms involved in transport of ciliary proteins to this region are not well understood.

Nephronophthisis (NPHP) represents a group of genetically heterogeneous renal cystic diseases that is associated with extrarenal manifestations such as retinitis pigmentosa, Leber congenital amaurosis, and cerebellar ataxia (Hildebrandt and Otto, 2000). Nephrocystin, the protein mutated in type I NPHP, localizes to the monocilia of polarized kidney epithelial cells (Otto *et al*, 2003). Recently, it has been demonstrated that renal monocilia are involved in mechanosensation (Praetorius and Spring, 2001; Nauli *et al*, 2003; Pazour and Witman, 2003).

Here we report that nephrocystin is expressed in ciliated respiratory epithelial cells and accumulates at the base of cilia, overlapping with markers of the basal body area and transition zone. Nephrocystin interacts and colocalizes with the transport protein phosphofurin acidic cluster sorting protein (PACS)-1. Casein kinase 2 (CK2)-mediated phosphorylation of nephrocystin is required for PACS-1 binding and nephrocystin targeting to the base of the cilia. Expression of a dominant-negative version of PACS-1 resulted in the loss of nephrocystin from the base of cilia. Therefore, these data suggest that CK2-dependent transport processes represent a novel pathway of targeting proteins to the base of the cilia.

Results

Nephrocystin is expressed in respiratory epithelial cells and accumulates at the base of the cilia

Prompted by the observation that patients with type I NPHP may experience an increased incidence of upper respiratory infections (H Omran, unpublished observation), we examined the expression and subcellular localization of nephrocystin in human nasal epithelial cells. Using an affinity-purified, highly specific anti-nephrocystin antibody

*Corresponding author. Renal Division, University Hospital, Hugstetterstrasse 55, 79106 Freiburg, Germany. Tel.: +49 761 270 3559; Fax: +49 761 270 3270; E-mail: thomas.benzing@uniklinik-freiburg.de
[5]These authors contributed equally to this work

Received: 29 June 2005; accepted: 3 November 2005; published online: 24 November 2005

(Benzing *et al*, 2001), we found that nephrocystin was abundantly expressed in respiratory cells (Figure 1A) and present in motile cilia (Figure 1B and C). The punctate pattern of nephrocystin staining in the ciliary axoneme closely resembled staining of nephrocystin in the monocilia of kidney cells (Otto *et al*, 2003). Confocal images revealed that nephrocystin, in addition to its weaker punctate cilial staining pattern, also intensively stained the base of cilia in respiratory epithelial cells, suggesting that this localization represents a pool of nephrocystin entering the ciliary compartment (Figure 1D). Costaining with markers of the ciliary axoneme (Figure 1D, left panel, antiacetylated tubulin) and of basal bodies (Figure 1D, right panel, anti-gamma-tubulin) provided further evidence that nephrocystin accumulated at the basal body and transition zone area of cilia. Although partially overlapping with gamma-tubulin staining, nephrocystin staining was detectable more apically (Figure 1D, right panel). This compartment has recently been shown to contain the retinitis pigmentosa guanosine phosphatase regulator (RPGR) (Hong *et al*, 2003). RPGR is mutated in hereditary retinitis pigmentosa, and interacts with nephrocystin-5, another NPHP disease protein (Otto *et al*, 2005). RPGR was present in human respiratory cells and colocalized with nephrocystin (Figure 2A). To confirm that nephrocystin localizes to the transition zone/basal body area of cilia, but not to other parts of the apical membrane, we partially disintegrated ciliated cells mechanically, and stained the disintegrated cilia for acetylated tubulin and nephrocystin. Single dots of nephrocystin staining, depicted in red, always delineated the origin of single disintegrated cilia, depicted in green,

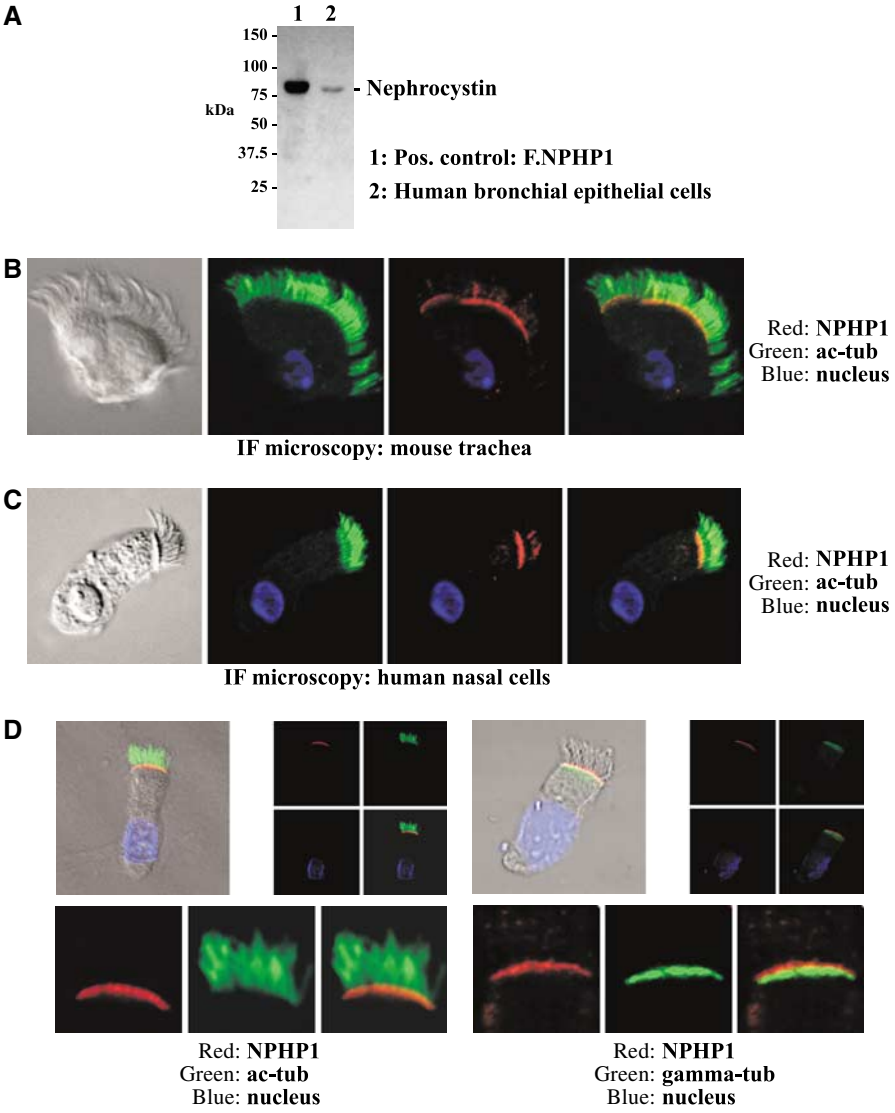

Figure 1 Nephrocystin is expressed in respiratory epithelial cells and accumulates at the base of cilia. (**A**) Lysates of HEK 293T cells transfected with FLAG-tagged NPHP1 (left lane) and human tracheal epithelial cells (right lane) were immunoblotted with an affinity-purified specific anti-nephrocystin antibody (Benzing *et al*, 2001) demonstrating nephrocystin expression in respiratory epithelial cells. (**B, C**) Conventional immunofluorescence microscopy of mouse tracheal cells (B) and human nasal epithelial cells (C) stained with a specific anti-nephrocystin antibody (Benzing *et al*, 2001) demonstrates distinct and punctate nephrocystin staining in the ciliary axoneme and a strong signal at the base of motile cilia of the respiratory tract (red). Cilia were visualized with antiacetylated tubulin antibody (green); blue, nuclei. (**D**) Confocal microscopy confirms intense staining for endogenous nephrocystin (red) at the base of cilia in human nasal epithelial cells. Staining for acetylated tubulin (green) is used to highlight the cilium. Nuclei are stained in blue (left panel). Double labelling for gamma-tubulin (green), a marker of the basal bodies, and nephrocystin (red) confirms accumulation of nephrocystin protein at the transition zone/basal body area (right panel).

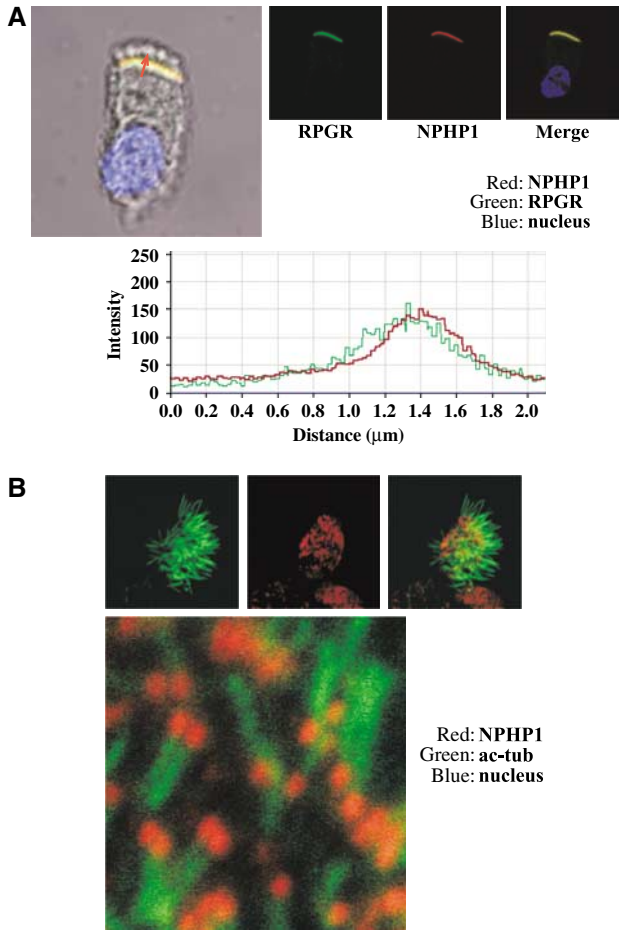

Figure 2 Colocalization of nephrocystin with RPGR at the transition zone/basal body area of cilia in human respiratory epithelial cells. (**A**) Staining of endogenous nephrocystin (red) and RGPR (green) in respiratory epithelial cells reveals colocalization of both proteins at the transition zone/basal body area of motile cilia. Nuclei (blue). Fluorescence signal intensities of nephrocystin (red) and RPGR (green), generated from a scanned horizontal line shown as red arrow in the merged image, are shown in the bottom panel. (**B**) Nephrocystin staining is confined to cilia and does not derive from other parts of the apical membrane. Cilia were disintegrated mechanically to show localization of nephrocystin at the base of each disintegrated cilium. Nephrocystin (red), acetylated tubulin (green), and nuclei (blue).

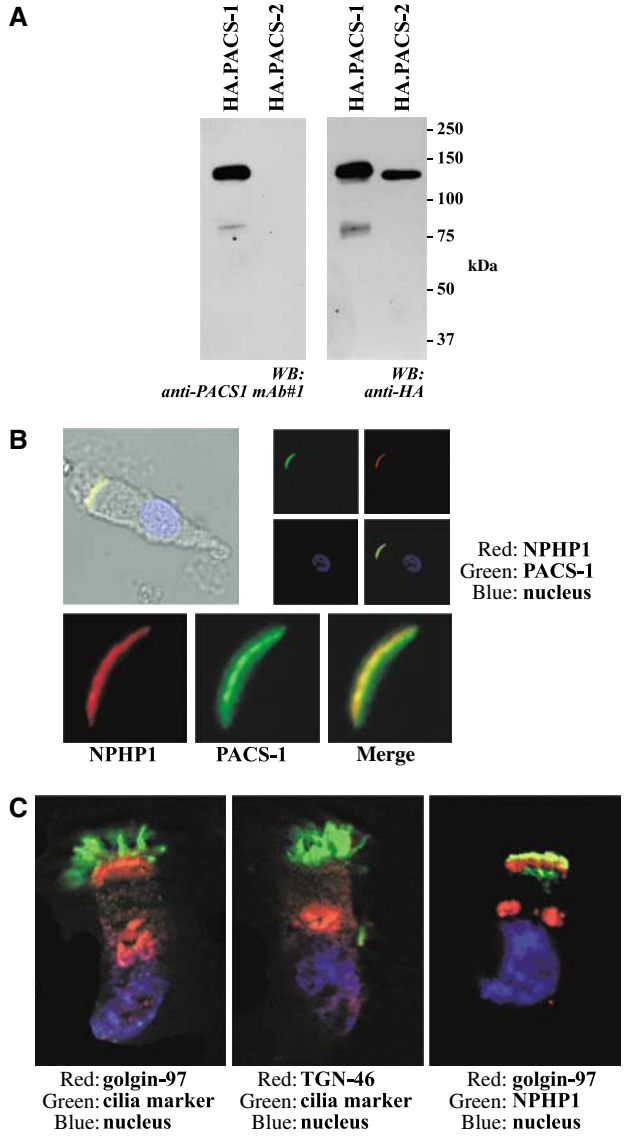

Figure 3 Nephrocystin colocalizes with the transport protein PACS-1 at the base of cilia of respiratory epithelial cells. (**A**) Monoclonal anti-PACS-1 antibody mAb#1 specifically recognizes HA-tagged PACS-1, but does not show crossreactivity with the related protein HA.PACS-2. HEK 293T cells were transfected with the plasmids as indicated. Lysates were prepared and immunoblotted with anti-PACS-1 antibody mAb#1 (left panel) as well as anti-HA antibody (right panel). (**B**) Colocalization of PACS-1 (green) with nephrocystin (red) at the base of the cilia. Nuclei (blue). Human nasal epithelial cells were isolated by brush biopsy and stained with anti-nephrocystin and anti-PACS-1 antibodies. (**C**) Native nasal epithelial cells were stained with anti-golgin-97 (Molecular Probes; left panel) and anti-TGN-46 antibody (Serotec; middle panel). Costaining with anti-NPHP1 antibody demonstrates that the base of the cilia is partially overlapping with a golgin-97-positive distinct domain of the secretory pathway (right panel).

confirming that nephrocystin staining is confined to the transition zone/basal body area in respiratory epithelial cells (Figure 2B) and not to other parts of the apical membrane. These data suggested that respiratory epithelial cells may represent a valid model system to study targeting of nephrocystin to the base of the cilia.

Nephrocystin associates with the phosphoacidic cluster sorting protein PACS-1

Nephrocystin is a multiadaptor protein and contains an SH3 domain that is flanked by two clusters of acidic residues harboring several potential CK2 phosphorylation sites. Clusters of aspartate or glutamate (acidic clusters) are required to bind the phosphoacidic cluster sorting protein PACS-1, a transport protein that has been shown to be involved in sorting the endopeptidase furin, the mannose-6-phosphate receptors (Wan *et al*, 1998), the R-SNARE VAMP4 (Hinners *et al*, 2003), the polycystin-2/TRPP2 cation channel (Kottgen *et al*, 2005), the viral proteins nef (Piguet *et al*, 2000; Blagoveshchenskaya *et al*, 2002), and cytomegalovirus glycoprotein B (Crump *et al*, 2003). To determine the localization of PACS-1 in respiratory epithelial cells, we raised a series of specific monoclonal antibodies against human PACS-1. Several clones including the one shown in Figure 3A (anti-PACS-1 mAb#1) specifically recognized PACS-1 without showing crossreactivity with the related PACS-2 protein.

Interestingly, staining of nasal epithelial cells with these antibodies revealed colocalization of PACS-1 with nephrocystin at the base of cilia (Figure 3B). While nephrocystin staining (in addition to its weaker staining in cilia) was confined to the transition zone/basal body area, PACS-1 showed a slightly more widespread distribution at the ciliary base. This area also stained positive with antibodies against golgin-97 (Figure 3C) (Yoshino *et al*, 2003; Derby *et al*, 2004), but was lacking reactivity for the TGN marker protein TGN-46. These data illustrated that the transition zone/basal body area may represent a previously ill-defined compartment in the secretory pathway, and suggested a possible role for PACS-1 in controlling the subcellular localization of ciliary proteins such as nephrocystin.

To investigate whether nephrocystin may interact with PACS-1, we generated a fusion construct of the furin-binding region (FBR) of PACS-1 with the CH2 and CH3 domains of human IgG (hIg.PACS-1^{85-280}), and coexpressed this construct in HEK 293T cells together with FLAG-tagged nephrocystin (F.NPHP1). The FBR mediates association with acidic clusters of various proteins (Wan *et al*, 1998; Scott *et al*, 2003). As demonstrated in Figure 4A, nephrocystin specifically co-precipitated with hIg.PACS-1^{85-280}, but not with the control construct lacking the FBR (hIg). This interaction could also be demonstrated in overlay assays, where we used the bacterially expressed and affinity-purified glutathione-*S*-transferase fusion protein of the FBR coupled to glutathione-linked horseradish peroxidase as a reagent to detect interaction with FLAG-tagged nephrocystin (Figure 4B). Pulldown assays confirmed the interaction (Figure 4C), and revealed that endogenous nephrocystin from mouse kidney was specifically immobilized by FBR fusion proteins (Figure 4D). Using the specific anti-PACS-1 and anti-nephrocystin antibodies, the interaction was demonstrated for endogenous proteins precipitated from mouse kidney lysates (Figure 4E), confirming that this interaction occurs *in vivo*.

Requisite phosphorylation of serines 121, 123, and 126 of nephrocystin mediates interaction with PACS-1

To map the PACS protein interaction site, we generated a series of truncations and deletion mutants of nephrocystin (Figure 5A). PACS-1 interaction required the acidic cluster of nephrocystin amino-terminal to the SH3 domain (Figure 5B). This acidic cluster contains at least four perfect consensus phosphorylation sites for CK2, and a bacterially expressed version of nephrocystin containing these serine residues was phosphorylated by CK2 *in vitro* (Figure 5C). Therefore, we speculated that phosphorylation of these serine residues is required for efficient binding of nephrocystin to PACS-1. To

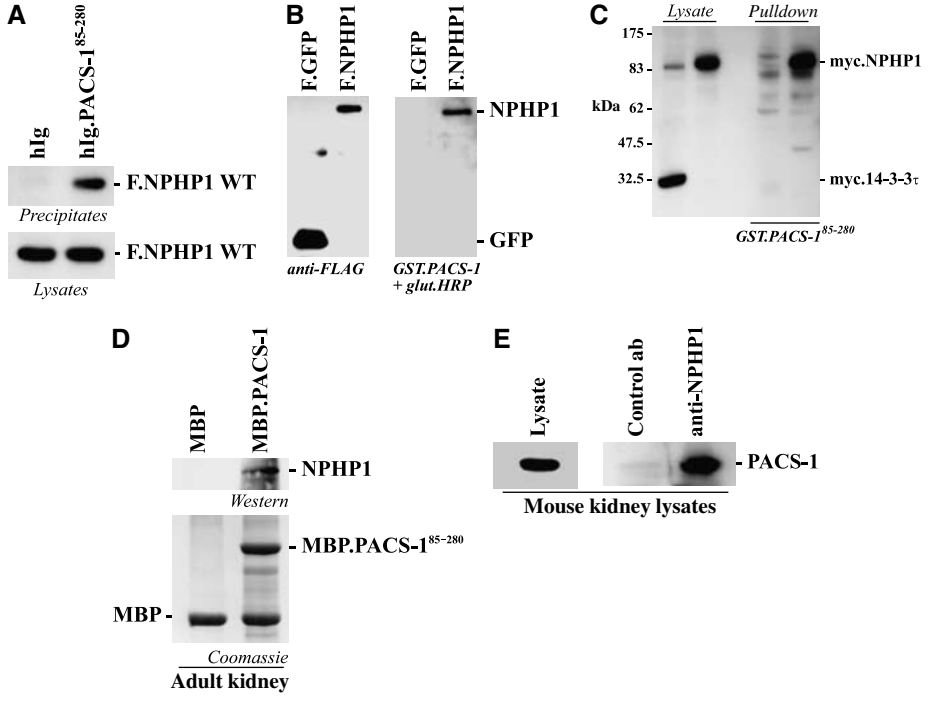

Figure 4 Nephrocystin interacts with acidic cluster sorting protein PACS-1. (**A**) Nephrocystin co-precipitates with PACS-1. Ig-tagged PACS-1 (amino acids 85–280) or a control protein and Flag-tagged nephrocystin (F.NPHP1) were expressed in HEK 293T cells and precipitated with protein G. Western blot analysis was performed with a FLAG-specific antibody (top). Expression levels of F.NPHP1 in the lysates are shown (bottom). (**B**) Lysates of cells expressing FLAG-tagged green fluorescent protein (F.GFP) or nephrocystin (F.NPHP1) were analyzed on Western blots with anti-FLAG antibody (left) or by overlay assays using a GST fusion protein of PACS-1 coupled to horseradish peroxidase as detection reagent (right panel). (**C**) Pulldown assays using a recombinant GST fusion protein of PACS-1 confirm specific interaction with nephrocystin. (**D**) Pulldown of endogenous nephrocystin from mouse kidney lysates (top). Protein lysates from mouse kidneys were incubated with recombinant MBP fusion proteins immobilized on beads. After incubation at 4°C, the beads were washed extensively and bound proteins were analyzed by immunoblotting. Co-precipitating endogenous nephrocystin protein is shown in the upper panel, expression of recombinant MBP fusion proteins is shown in the lower panel. (**E**) Endogenous nephrocystin interacts with PACS-1 in the kidney, suggesting that the interaction occurs *in vivo*. Protein lysates from mouse kidneys were subjected to immunoprecipitation with a control antibody (second lane) or specific anti-nephrocystin antibody (third lane), washed extensively and immunoblotted with specific anti-PACS-1 antibody. The first lane depicts PACS-1 expression in the kidney lysate.

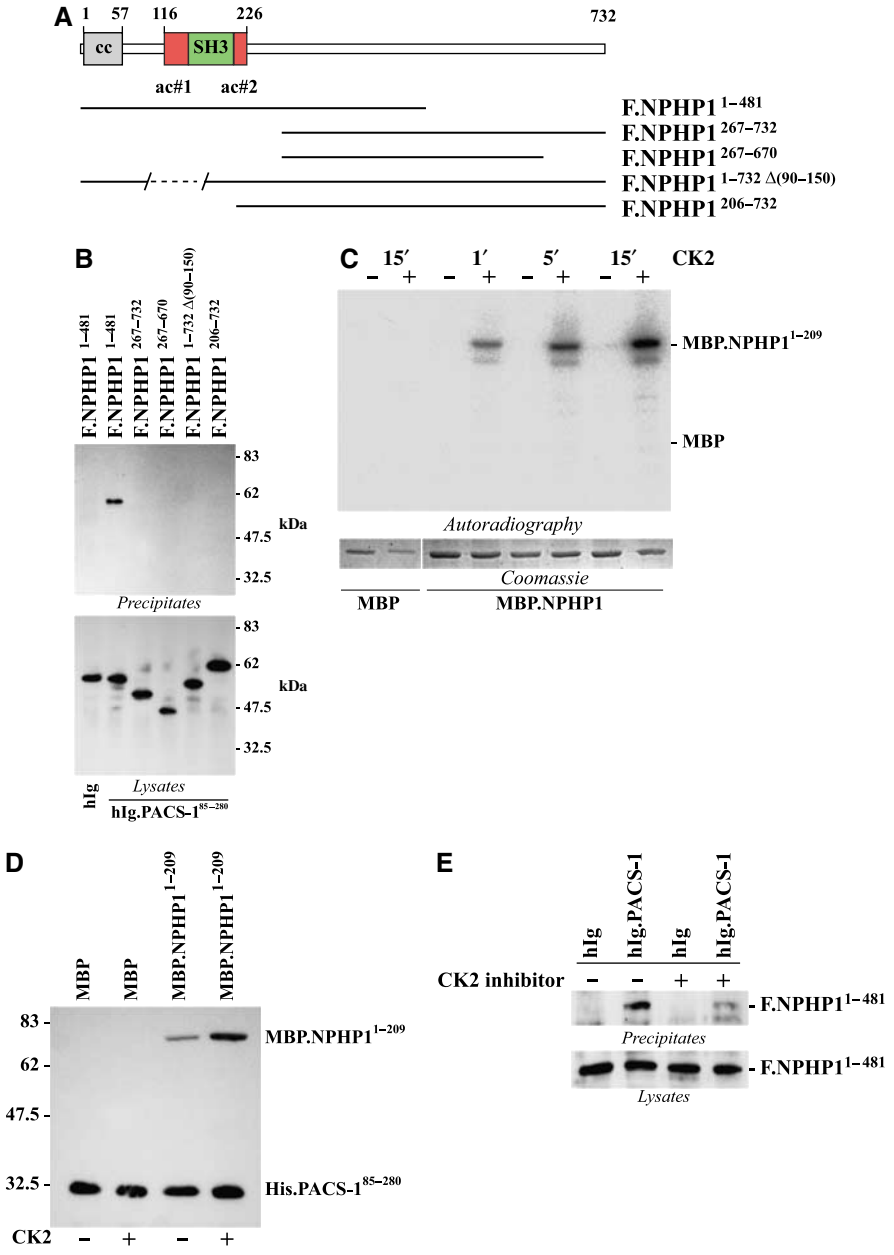

Figure 5 The interaction between nephrocystin and PACS-1 is phosphorylation-dependent and maps to a cluster of acidic residues in nephrocystin. (**A**) Several Flag-tagged nephrocystin truncations were generated to analyze the interaction with PACS-1. The SH3 domain in nephrocystin (green) is flanked by two clusters of acidic residues (red). (**B**) PACS-1 interaction requires a region of nephrocystin that contains the first acidic cluster (top). HEK 293T cells were cotransfected with Ig-tagged PACS-1 (amino acids 85–280) and FLAG-tagged nephrocystin constructs as indicated. Ig-tagged PACS-1 was precipitated with protein G and the precipitates were analyzed for co-precipitating nephrocystin truncations (upper panel). Expression levels of FLAG-tagged nephrocystin constructs are shown (bottom). Expression level of hIg.PACS-1 was identical in all cell lysates (not shown). (**C**) A bacterially expressed recombinant fusion protein of nephrocystin (MBP.NPHP1) containing the first acidic cluster (amino acids 1–209) is time-dependently phosphorylated by CK2. Autoradiograph after *in vitro* phosphorylation of MBP or MBP.NPHP1 with CK2 (top). Expression of recombinant fusion proteins is shown (bottom). (**D**) *In vitro* interaction of His.PACS-1^{85-285} with MBP (before and after treatment with CK2, lanes 1 and 2) and MBP.NPHP1^{1-209} (before and after treatment with CK2, lanes 3 and 4) shows dependence of the interaction on CK2 activity. His-tagged PACS-1 (amino acids 85–280) was bound to Ni^{+} beads and incubated with equal amounts of MBP (first two lanes) or MBP.NPHP1 (amino acids 1–209) preincubated or not preincubated with CK2. Ni^{+} beads were washed extensively and analyzed for co-precipitating MBP fusion proteins with anti-MBP antibody. His-tagged PACS-1 was visualized by reprobing the blot with anti-His antibody. (**E**) Treatment of cells with the CK2 inhibitor TBB (20 μM, 4 h) prior to cell lysis inhibits the interaction of PACS-1 with nephrocystin (upper panel). Expression levels are shown (lower panel). Equal expression of Ig-tagged proteins was confirmed by reprobing with anti-human-IgG antibody (not shown).

address this hypothesis, we mutated these serine residues to alanines that abrogated phosphorylation (not shown). Consistently, CK2 phosphorylation of nephrocystin dramatically augmented binding of PACS-1, as shown by *in vitro* interaction experiments (Figure 5D), whereas inhibition of CK2 with the specific inhibitor 4,5,6,7-tetrabromo-2-azabenzimidazole (TBB, 20 μM, 4 h) abrogated the interaction in coimmunoprecipitation experiments (Figure 5E). To identify the phosphorylated amino acids *in vivo*, we labelled cells expressing wild-type nephrocystin and performed complete

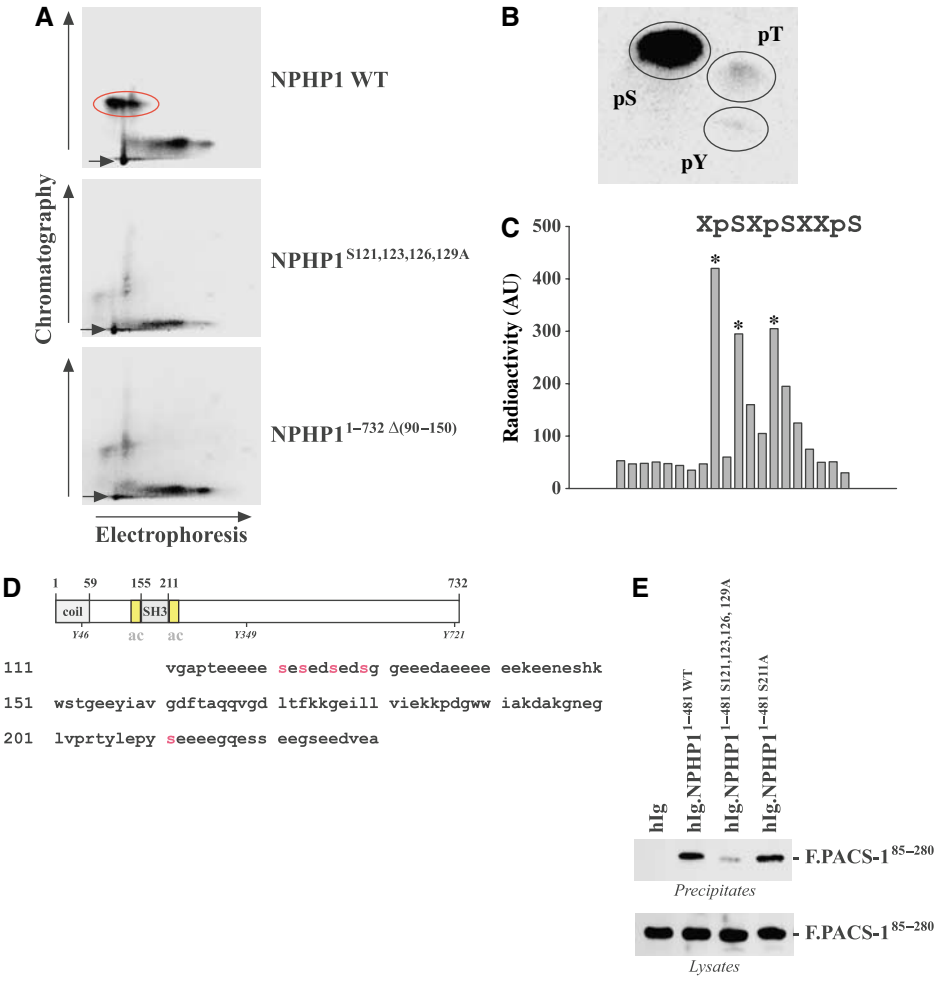

Figure 6 Requisite phosphorylation of serines 121, 123, 126, but not serine 129, of nephrocystin mediates interaction with PACS-1. (**A**) Radioactive labelling, followed by precipitation of nephrocystin, completes tryptic digest of the protein, and two-dimensional separation of the peptide fragments reveals a major phosphopeptide in wild-type nephrocystin that is absent in the serine-to-alanine mutants lacking serine 121, 123, 126, and 129, as well as in the deletion mutant of the first acidic cluster of nephrocystin. (**B**) The indicated peptide was eluted and a fraction was hydrolyzed and subjected to phosphoamino-acid analysis (locations of standard phosphoamino acids are indicated by black circles, pS-phospho-serine, pT-phospho-threonine, pY-phospho-tyrosine). (**C**) The remaining portion of the eluted phosphopeptide was subjected to 20 cycles of Edman degradation and cleaved amino acids were collected and analyzed using a PhosphorImager to locate the position of the phosphorylation site(s). The content of ^{32}P radioactivity of each sequencing cycle is expressed in arbitrary units (AU). (**D**) The SH3 domain of nephrocystin (highlighted in gray) is flanked by two acidic clusters (yellow) containing putative CK2 phosphorylation sites (red). (**E**) Mutation of the CK2 phosphorylation sites in nephrocystin to alanines prevents binding of PACS-1. HEK 293T cells were transfected with the plasmids as indicated and subjected to precipitation with protein G, followed by immunoblotting with anti-FLAG antibody. The lower panel shows expression in the lysates.

tryptic digest. Phosphoamino-acid analysis of precipitated nephrocystin revealed two major phosphopeptides (Figure 6A, upper panel). The major phosphorylated peptide was absent in a mutated nephrocystin lacking the serine residues of the acidic cluster (Figure 6A, middle panel), or a deletion mutant lacking the entire region (Figure 6A, lower panel), demonstrating that these serine residues of nephrocystin are phosphorylated *in vivo*. Total hydrolysis and phosphoamino-acid analysis performed on the isolated spot demonstrated that this peptide contained exclusively phosphoserine, but no phosphorylated tyrosines or threonines (Figure 6B). The major fraction of the peptide was used for solid-phase Edman degradation, revealing a pattern of **x*x*xx*xxxxx** ('*' representing a radioactively labelled residue, and '**x**' a nonlabelled amino acid) (Figure 6C). Comparison to the predicted fragments resulting from tryptic digest (www.expasy.org/tools/peptide-mass.html) revealed that this fragment corresponded to a peptide containing parts of the first acidic cluster, indicating that Ser121, Ser123, and Ser126, but not Ser 129, were phosphorylated *in vivo*. Consistently, serine-to-alanine mutation of these residues dramatically decreased binding of PACS-1 to nephrocystin, as depicted in Figure 6E, further supporting our concept that efficient PACS-1 binding to nephrocystin requires CK2-dependent serine phosphorylation within the acidic cluster of nephrocystin.

CK2-dependent phosphorylation of nephrocystin is required for localization to the transition zone of cilia

PACS-1 has been identified as a sorting connector, which retrieves membrane-associated proteins to TGN and endosomes (Wan *et al*, 1998; Crump *et al*, 2001). These processes are regulated through CK2-dependent protein interactions of cargo proteins with PACS-1. To demonstrate that CK2-

mediated phosphorylation affects nephrocystin localization, we incubated freshly isolated native human nasal epithelial cells with the highly selective CK2 inhibitor 2-dimethylamino-4,5,6,7-tetrabromo-1H-benzimidazole (DMAT) (1.5 μM, 2 h at 37°C). CK2 inhibition with DMAT resulted in the loss of nephrocystin from the base of cilia (Figure 7A) without affecting cilia morphology or antiacetylated tubulin staining. Instead of localizing to the transition zone/basal body area, nephrocystin assumed a vesicle-like subcellular distribution. This was associated with an almost complete loss of nephrocystin staining in the ciliary axonemes. Similar results were obtained with the CK2 inhibitors 5,6-dichloro-1-β-D-ribofuranosyl-benzimidazole (DRB) and TBB (not shown), demonstrating that nephrocystin localization to the transition zone is critically dependent on CK2 activity. To further investigate the role of PACS-1 for targeting nephrocystin to the transition zone, we next used a vaccinia virus to express a dominant-negative version of PACS-1 (PACS-1 ADMUT; Crump *et al*, 2001) in respiratory epithelial cells. Transduction of mouse trachea in primary culture resulted in expression of HA-tagged PACS-1 ADMUT already 4 h after infection (Figure 7B). Respiratory epithelial cells were harvested 16 h after the infection with either control vaccinia virus or PACS-1 ADMUT vaccinia virus, and stained with antiacetylated tubulin and antinephrocystin antibody. Expression of PACS-1 ADMUT resulted in the loss of nephrocystin from the transition zone, whereas the control vaccinia virus was without effect. Taken together, these data demonstrated that phosphorylation-dependent PACS-1 interaction is required for the targeting of nephrocystin to the base of cilia.

Discussion

Recent evidence has suggested that proteins that reside in the cilia of various cell types are involved in the development of a large number of diseases ranging from cystic kidney and retinal degenerative disease to liver fibrosis, bone abnormalities, and diabetes. Although of critical importance for human disease, very little is known regarding how these proteins are targeted to the ciliary compartment.

Here, we show that nephrocystin, a prototypical member of this family of cilia-associated proteins, interacts with the phosphoacidic cluster sorting protein PACS-1. CK2-mediated phosphorylation of three critical serine residues within a cluster of acidic amino acids in nephrocystin was required for PACS-1 binding and targeting of nephrocystin to the transition zone/basal body region of cilia. PACS-1 has been implicated in trafficking of a variety of cellular proteins and targeting of proteins to the TGN and the endosomal compartment. Thus, it was surprising to see that in respiratory epithelial cells PACS-1 specifically localized at the ciliary base. This area stained positive for both PACS-1 and golgin-97, a peripheral membrane protein that has been shown to localize to a distinct domain of the TGN in unpolarized cells

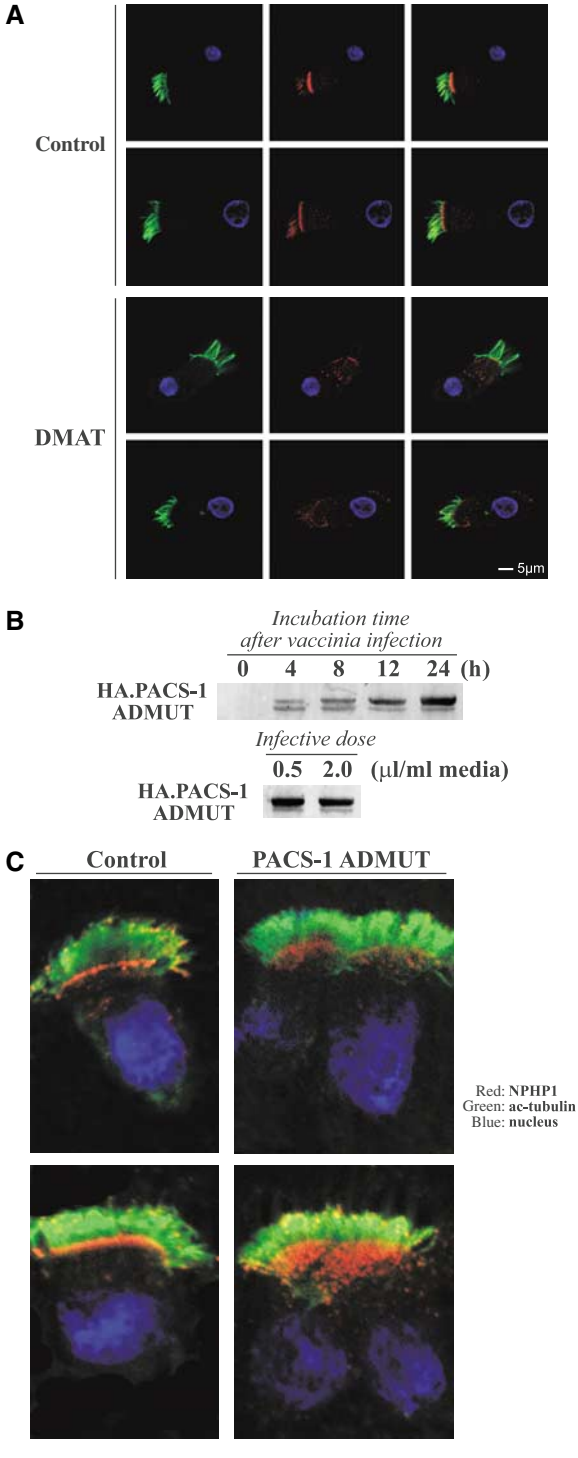

Figure 7 Targeting of nephrocystin to the transition zone/basal body area requires CK2 activity and is dependent on PACS-1. (**A**) Native human respiratory epithelial cells, freshly isolated by brush biopsy, were incubated with solvent (upper panels) or the highly selective CK2 inhibitor DMAT (1.5 μM, 2 h at 37°C) (lower panels), fixated in paraformaldehyde (4%) and stained for nephrocystin (red) and acetylated tubulin (green). Nuclei (blue). Instead of localizing to the transition zone/basal body area as shown in solvent-treated cells (upper panel), nephrocystin assumes a vesicle-like subcellular distribution (lower panel). (**B**) Vaccinia virus-mediated expression of a dominant-negative mutant of PACS-1 (PACS-1 ADMUT) in mouse trachea. Time- and dose-dependent expression of PACS-1 ADMUT was analyzed on immunoblots of mouse tracheal cells with anti-HA antibody. (**C**) Expression of PACS-1 ADMUT results in loss of nephrocystin from the ciliary base. Respiratory epithelial cells were harvested 16 h after the infection with either control vaccinia virus (Control) or PACS-1 ADMUT vaccinia virus (PACS-1 ADMUT) and stained with antiacetylated tubulin and anti-nephrocystin antibody.

(Yoshino *et al*, 2003; Derby *et al*, 2004). Although cross-reactivity with another closely related protein cannot be excluded, these data suggest that distal parts of the TGN are in close connection with the base of the cilia. Alternatively, these data may suggest that the base of cilia is part of a novel, previously undefined golgin-97- and PACS-1-positive compartment that is distinct from the TGN. Both explanations are in agreement with electron microscopy studies revealing that parts of the TGN and endosomes reach the apical surface in ciliated epithelial cells (for a review of 'cilia/flagella and transport', see Pazour and Rosenbaum, 2002; Rosenbaum and Witman, 2002). Our results link established cellular transport mechanisms with the targeting of ciliary proteins and have several important implications. First, acidic cluster domains similar to the one identified in nephrocystin can be found in a variety of proteins involved in cilia-related human disease. These proteins include the cystic kidney disease proteins polycystin-2, the Bardet Biedl syndrome protein BBS2, and others. Therefore, CK2-dependent transport processes involving binding to the transport protein PACS-1 may represent a more general mechanism for targeting of proteins to the base of cilia. Second, this study identifies nephrocystin as a component of the motile cilia of respiratory epithelial cells. Interestingly, cystic kidney disease patients can present with respiratory symptoms consistent with possible respiratory ciliary defects. This study may initiate a search for a subtle respiratory phenotype in NPH patients. Third, the localization of nephrocystin to the transition zone/basal body area of cilia suggests a possible role of nephrocystin in controlling access of other proteins to the ciliary compartment. Although cilia and flagella are ostensibly open to the cytoplasm, it seems that only a subset of cytoplasmic proteins is admitted to the ciliary/flagellar compartment. In *Chlamydomonas reinhardtii*, the boundary between the cytoplasmic and flagellar compartments is demarcated by transition fibers, which extend from the distal end of the basal body and connect each of the nine basal-body triplet microtubules to the flagellar membrane (Rosenbaum and Witman, 2002). Rosenbaum and Witman (2002) proposed that these transition fibers might be structural components of a flagellar pore complex (FPC) that controls the movement of molecules and particles between the cytoplasmic and flagellar compartments, much as the nuclear pore controls movement between the cytoplasmic and nuclear compartments. Immunoelectron microscopy has shown that the transition fibers are docking sites for the intraflagellar transport particle proteins at the base of the flagellum. Interestingly, in photoreceptors, the transition zone is formed by the connecting cilium of rods and cones (Hong *et al*, 2003; Snell *et al*, 2004). Diseased protein transport in the connecting cilium of photoreceptors results in retinal degeneration, which can also be found in NPHP patients (Deretic and Papermaster, 1991; Pazour *et al*, 2002). Thus, loss of nephrocystin from the transition zone/basal body area may represent a common pathomechanism for cystic kidney disease as well as respiratory disorders and retinitis pigmentosa in NPHP patients. In the nematode *Caenorhabditis elegans*, ciliated sensory neurons located in the head and tail sense an extensive variety of environmental signals and mediate a wide spectrum of actions. The male possesses ciliated neurons primarily involved in male mating behavior. Interestingly, NPHP1 is required for male sensory behaviors (Jauregui and Barr, 2005). GFP-tagged NPHP1 and NPHP4 proteins localized to ciliated sensory endings of dendrites in male-specific sensory cilia. *nphp1;nphp4* double mutant males had intact cilia, but were response defective, suggesting a role for NPHP1 and NPHP4 in ciliary sensory signal transduction. To exert their action, these proteins have to localize to the sensory organelles, to the base of cilia. Thus, it is highly conceivable that trafficking defects may be involved in the pathogenesis of NPHP1-related disease.

Together, these data suggest a critical role for CK2 and PACS-1 in controlling access/transport of proteins destined to reach cilia. Based on these data, one may expect that a deeper understanding of the transport mechanisms involved in targeting to the ciliary base as well as the physiological function subserved by nephrocystin and PACS-1 will be discernable by studying trafficking in ciliated respiratory epithelial cells.

Materials and methods

Plasmids and antibodies

Nephrocystin and PACS-1 constructs have been described previously (Benzing *et al*, 2001; Kottgen *et al*, 2005). HA-tagged versions of human PACS-1 were generously provided by Dr G Thomas (Vollum Institute, Portland/Oregon). Fusion proteins of the FBR of PACS-1 were generated by PCR cloning using a pCDM8 cassette that contained the leader sequence of CD5 fused to the CH2 and CH3 domains of human IgG_1, followed by a cloning cassette (kindly provided by Dr B Seed, Harvard Medical School, Boston, MA) (Tsiokas *et al*, 1997). Site-directed mutagenesis was performed using the QuickChange Site-Directed Mutagenesis Kit (Stratagene). All plasmids were verified by automated DNA sequencing. Antibodies were obtained from Sigma (anti-FLAG, antiacetylated tubulin), Santa Cruz (anti-myc, anti-HA, anti-RPGR), Roche Biochemicals (anti-HA), Serotec (anti-TGN-46), Molecular Probes (anti-golgin-97), and Upstate Biotechnologies (anti-PY 4G10). Vaccinia viruses expressing PACS-1 ADMUT were kindly provided by Dr G Thomas (Vollum Institute, Portland, OR). These viruses as well as control virus were produced as described previously (Wan *et al*, 1998; Crump *et al*, 2001).

Cell culture and transfections

HEK 293T cells were cultured in DMEM supplemented with 10% fetal bovine serum. For transfection experiments, cells were grown until 60–80% confluence and transfected with plasmid DNA using a modified calcium phosphate method as described previously (Benzing *et al*, 1999, 2000). At 24 h after transfection, cells were lysed in 1 ml/10-cm dish of ice-cold lysis buffer (1% Triton X-100, 20 mM Tris–HCl, pH 7.5, 50 mM NaCl, 50 mM NaF, 15 mM $Na_4P_2O_7$, 2 mM Na_3VO_4 and protease inhibitors) for 15 min on ice. Lysates were centrifuged at 4°C for 15 min at 14 000 r.p.m., and subsequently subjected to ultracentrifugation (100 000 *g*, 30 min, 4°C). Supernatants were used for *in vitro* binding assay, affinity purification and coimmunoprecipitation studies.

Coimmunoprecipitation

Coimmunoprecipitations were performed as described (Huber *et al*, 2003). For precipitation of endogenous proteins, mouse kidneys were perfused *in situ* with ice-cold phosphate-buffered saline (PBS) and homogenized in 2 ml of lysis buffer (20 mM Tris–HCl, pH 7.5/1% Triton X-100/25 mM NaF/12.5 mM $Na_4P_2O_7$/0.1 mM EDTA/50 mM NaCl/2 mM Na_3VO_4 and protease inhibitors). After centrifugation to remove cellular debris, the supernatant was subjected to an ultracentrifugation (100 000 *g*) for 30 min, followed by extensive preclearing with protein G Sepharose. Immunoprecipitation with control antibody or anti-nephrocystin antiserum was performed as described (Benzing *et al*, 2001). Briefly, 50 µl was kept as lysate and the rest (1 ml) was divided into two portions and subjected to immunoprecipitation with 2 µg of control or nephrocystin antibody and protein G beads. Precipitates were washed extensively and analyzed for co-precipitating proteins.

Pulldown assay

HEK 293T cells were transiently transfected with plasmid DNA as indicated. After stimulation, cells were lysed in ice-cold lysis buffer. Following centrifugation, the supernatant was incubated for 1 h at 4°C with 2 μg of recombinant purified glutathione-*S*-sepharose (GST), histidine-tag, or maltose-binding-protein (MBP) fusion proteins prebound to glutathione-Sepharose (Amersham Biosciences), nickel beads (Qiagen), or amylose resin (New England Biolabs) as indicated. Bound proteins were separated by SDS–PAGE, and precipitated proteins were visualized by immunoblotting with anti-FLAG and anti-myc antibodies. Equal loading of fusion proteins was confirmed by Coomassie Blue staining of the gels. For pulldown assays of endogenous proteins, kidney lysates were prepared as described above.

In vitro phosphorylation and interaction

In vitro phosphorylation of MBP.NPHP1$^{1-209}$ was performed for 30 min at 25°C in a 100-μl reaction in a buffer containing 20 mM Tris–HCl, 50 mM KCl, 10 mM $MgCl_2$, pH 7.5, 100 μM ATP (with or without γ-^{32}P-ATP). The phosphorylation was initiated by the addition of 1.0 U of recombinant CK2 (New England Biolabs) in enzyme dilution buffer or enzyme dilution buffer alone (control). To monitor the incorporation of phosphate, the unlabelled ATP was supplemented with 10 μCi of γ-^{32}P-ATP, and radiolabelled MBP.NPHP1$^{1-209}$ was visualized by SDS–PAGE and autoradiography. For *in vitro* interaction studies, purified recombinant protein (1 μg of phosphorylated (through CK2) or unphosphorylated MBP.NPHP1$^{1-209}$ or MBP alone) was incubated with 2.5 μg recombinant His.PACS-1$^{85-280}$ immobilized on Ni^+ beads for 90 min in 450 μl of binding buffer containing 50 mM potassium phosphate, pH 7.5, 150 mM KCl, 1 mM $MgCl_2$, 10% (v/v) glycerol, 1% Triton X-100, and protease inhibitors. The washed precipitate was separated on a 10% SDS acrylamide gel. Bound MBP.NPHP1$^{1-209}$ was detected by immunoblotting using an anti-MBP rabbit antiserum (New England Biolabs). His.PACS-1$^{85-280}$ was counterstained with monoclonal anti-His antibodies (Qiagen, Germany). DRB (30 μM final concentration) was purchased from Alexis (Germany); DMAT and TBB (20 μM final concentration) were purchased from Calbiochem.

Generation and purification of a PACS-1-specific monoclonal antibody

A bacterially expressed and affinity-purified His-tagged PACS-1 fragment (His.PACS-1$^{85-280}$) was used to immunize mice following a standard immunization protocol (Kohler and Milstein, 1975). Fusions resulted in the generation of more than 20 specific monoclonal antibodies that were subcloned and typed as mouse IgG1. Protein A/G columns were used to concentrate the PACS-1-specific antibodies. Specificity was verified by using bacterially expressed recombinant proteins, cell lysates from transfected cells, and homogenized renal tissue.

^{32}P labelling and two-dimensional mapping of phosphorylation sites

^{32}P labelling of cells (1–2 mCi/ml for 6–8 h), solubilization, and immunoprecipitation of nephrocystin were performed as described previously (Blaukat *et al*, 2001; Kruljac-Letunic *et al*, 2003). All experiments were performed in six-well plates. After separation of the immunoprecipitated proteins by 10% SDS–PAGE, the proteins were transferred onto nitrocellulose membranes. Radiolabelled proteins were detected by PhosphorImager (BAS2000, Fuji) analysis and tryptic digests were performed as described previously with minor modifications (Blaukat *et al*, 2001). Briefly, membrane pieces containing the ^{32}P-labelled proteins were cut out and blocked with 0.5% polyvinylpyrrolidone 40 in 0.6% acetic acid, for 30 min at 37°C. Following extensive washes with water, membrane-bound nephrocystin was cleaved *in situ* with sequencing grade trypsin in 50 mM $(NH_4)HCO_3$ for 12 h at 37°C. Released tryptic peptides were vacuum-dried and oxidized with performic acid for 1 h on ice. Reactions were stopped by dilution with 20% (v/v) ammonia solution. Thereafter, samples were frozen, vacuum-dried, and a second digest was performed for 12 h at 37°C. Following vacuum drying, samples were dissolved in electrophoresis buffer (formic acid:acetic acid:water, 46:156:1790 (v/v/v)) and phosphopeptides were separated by electrophoresis on cellulose thin-layer plates in a first dimension (2000 V, 40 min, electrophoresis buffer) and ascending chromatography in a second dimension (15 h, isobutyric acid, 1-butanol, pyridine, acetic acid, water, 1250:38:96:58:558 (v/v/v/v/v)). Phosphopeptides were detected by PhosphorImager analysis and eluted from the cellulose matrix with 20% (v/v) acetonitrile in a sonicated water bath for 15 min. Part of the extract (25–100 c.p.m.) was hydrolyzed with 6 M HCl for 1 h at 110°C and subjected to a phosphoamino-acid analysis. The second fraction (50–500 c.p.m.) was sequenced by Edman degradation using a solid-phase sequencer (ABI 477). In all, 20 sequencing cycles were collected, dried, and analyzed for their content of ^{32}P radioactivity using a PhosphorImager. Data obtained from Edman degradation were used to predict phosphorylation sites. The prediction was verified by *in vitro* mutagenesis of corresponding phosphoacceptor sites.

Immunofluorescence staining of respiratory epithelial cells

Human respiratory epithelial cells were obtained by transnasal brush biopsy using a cytobrush plus (Medscand Malmö, Sweden) and suspended in RPMI1640 without supplements. Samples were spread onto glass slides. Cells were fixed with 4% paraformaldehyde in PBS for 15 min and permeabilized with 0.2% Triton-X 100 in PBS for 5 min prior to blocking with 0.5% skim milk in PBS overnight. Cells were incubated with primary antibodies for 5 h and for 30 min with secondary antibody at room temperature. Antibodies were diluted in 0.5% skim milk and slides were washed 3–4 times with PBS after each step. Appropriate controls were performed omitting the primary antibodies. DNA was stained with 10 μg/ml Hoechst 33342 (Sigma) in H_2O. Images were taken on a Zeiss laser scan confocal microscope (LSM 510 iUV) and Zeiss microscopes equipped with the Apotome Imaging System.

Mouse trachea primary culture

Tracheas from female Balb/C mice (8–12 weeks) were aseptically dissected, collected in DMEM containing 20 mM HEPES, pH 7.4, and cut into half rings of the length of 3–4 rings of cartilage. These rings were placed ciliated site up within a cell culture insert on a 0.4 μm polyester membrane (Transwell, Corning). The remaining media around the tissue was partially removed with a micropipette. The outer site of the transwell plate was filled with 1 ml DMEM:F12 (1:1) supplemented with 10% Nu-Serum (Becton Dickinson), 1% fungizone (Invitrogen), and antibiotics (50 U/ml penicillin and 50 μg/ml streptomycin, Invitrogen). This technique avoids submersion of the ciliated areas, while still providing nutrients to the tissue. After culture times of up to 6 days (37°C, 5% CO_2), the epithelium showed a normal morphology with intact and beating cilia. Infection of the cultures with vaccinia virus was performed as described (Wan *et al*, 1998) immediately after preparation of the tracheal rings. To harvest ciliated respiratory epithelial cells, the epithelium was scraped in PBS with a scalpel, cells were collected by centrifugation, resuspended in a very small volume of DMEM, spread onto glass slides pretreated with Cell Tak (BD Biosciences), air dried, fixed with 4% PFA, permeabilized with 0.1% TX-100, blocked in 0.5% milk overnight, and stained as described above.

Acknowledgements

We thank Christina Engel, Stefanie Keller, Charlotte Meyer, and Petra Dämisch for excellent technical assistance, and members of the Benzing laboratory for helpful discussions. We thank Dr Roland Nitschke and the members of the Life Imaging Center Freiburg for expert technical advice and Dr Brian Seed and Dr Ivan Dikic for providing cDNAs. We are very grateful to Dr Gary Thomas for providing cDNAs and vaccinia viruses. This study was supported by DFG grants BE 2212, WA 517, and SFB592.

References

Ansley SJ, Badano JL, Blacque OE, Hill J, Hoskins BE, Leitch CC, Kim JC, Ross AJ, Eichers ER, Teslovich TM, Mah AK, Johnsen RC, Cavender JC, Lewis RA, Leroux MR, Beales PL, Katsanis N (2003) Basal body dysfunction is a likely cause of pleiotropic Bardet–Biedl syndrome. *Nature* **425:** 628–633

Benzing T, Brandes R, Sellin L, Schermer B, Lecker S, Walz G, Kim E (1999) Upregulation of RGS7 may contribute to tumor necrosis factor-induced changes in central nervous function. *Nat Med* **5:** 913–918

Benzing T, Gerke P, Hopker K, Hildebrandt F, Kim E, Walz G (2001) Nephrocystin interacts with Pyk2, p130(Cas), and tensin and triggers phosphorylation of Pyk2. *Proc Natl Acad Sci USA* **98:** 9784–9789

Benzing T, Yaffe MB, Arnould T, Sellin L, Schermer B, Schilling B, Schreiber R, Kunzelmann K, Leparc GG, Kim E, Walz G (2000) 14-3-3 interacts with regulator of G protein signaling proteins and modulates their activity. *J Biol Chem* **275:** 28167–28172

Blagoveshchenskaya AD, Thomas L, Feliciangeli SF, Hung CH, Thomas G (2002) HIV-1 Nef downregulates MHC-I by a PACS-1- and PI3K-regulated ARF6 endocytic pathway. *Cell* **111:** 853–866

Blaukat A, Pizard A, Breit A, Wernstedt C, Alhenc-Gelas F, Muller-Esterl W, Dikic I (2001) Determination of bradykinin B2 receptor *in vivo* phosphorylation sites and their role in receptor function. *J Biol Chem* **276:** 40431–40440

Calvet JP (2002) Cilia in PKD—letting it all hang out. *J Am Soc Nephrol* **13:** 2614–2616

Crump CM, Hung CH, Thomas L, Wan L, Thomas G (2003) Role of PACS-1 in trafficking of human cytomegalovirus glycoprotein B and virus production. *J Virol* **77:** 11105–11113

Crump CM, Xiang Y, Thomas L, Gu F, Austin C, Tooze SA, Thomas G (2001) PACS-1 binding to adaptors is required for acidic cluster motif- mediated protein traffic. *EMBO J* **20:** 2191–2201

Derby MC, van Vliet C, Brown D, Luke MR, Lu L, Hong W, Stow JL, Gleeson PA (2004) Mammalian GRIP domain proteins differ in their membrane binding properties and are recruited to distinct domains of the TGN. *J Cell Sci* **117:** 5865–5874

Deretic D, Papermaster DS (1991) Polarized sorting of rhodopsin on post-Golgi membranes in frog retinal photoreceptor cells. *J Cell Biol* **113:** 1281–1293

Hiesberger T, Igarashi P (2005) Elucidating the function of primary cilia by conditional gene inactivation. *Curr Opin Nephrol Hypertens* **14:** 373–377

Hildebrandt F, Otto E (2000) Molecular genetics of nephronophthisis and medullary cystic kidney disease. *J Am Soc Nephrol* **11:** 1753–1761

Hinners I, Wendler F, Fei H, Thomas L, Thomas G, Tooze SA (2003) AP-1 recruitment to VAMP4 is modulated by phosphorylation-dependent binding of PACS-1. *EMBO Rep* **4:** 1182–1189

Hong DH, Pawlyk B, Sokolov M, Strissel KJ, Yang J, Tulloch B, Wright AF, Arshavsky VY, Li T (2003) RPGR isoforms in photoreceptor connecting cilia and the transitional zone of motile cilia. *Invest Ophthalmol Vis Sci* **44:** 2413–2421

Huber TB, Hartleben B, Kim J, Schmidts M, Schermer B, Keil A, Egger L, Lecha RL, Borner C, Pavenstadt H, Shaw AS, Walz G, Benzing T (2003) Nephrin and CD2AP associate with phosphoinositide 3-OH kinase and stimulate AKT-dependent signaling. *Mol Cell Biol* **23:** 4917–4928

Ibanez-Tallon I, Heintz N, Omran H (2003) To beat or not to beat: roles of cilia in development and disease. *Hum Mol Genet* **12** (Spec No 1)**:** R27–R35

Igarashi P, Somlo S (2002) Genetics and pathogenesis of polycystic kidney disease. *J Am Soc Nephrol* **13:** 2384–2398

Jauregui AR, Barr MM (2005) Functional characterization of the *C. elegans* nephrocystins NPHP-1 and NPHP-4 and their role in cilia and male sensory behaviors. *Exp Cell Res* **305:** 333–342

Kohler G, Milstein C (1975) Continuous cultures of fused cells secreting antibody of predefined specificity. *Nature* **256:** 495–497

Kottgen M, Benzing T, Simmen T, Tauber R, Buchholz B, Feliciangeli S, Huber TB, Schermer B, Kramer-Zucker A, Hopker K, Simmen KC, Tschucke CC, Sandford R, Kim E, Thomas G, Walz G (2005) Trafficking of TRPP2 by PACS proteins represents a novel mechanism of ion channel regulation. *EMBO J* **24:** 705–716

Kruljac-Letunic A, Moelleken J, Kallin A, Wieland F, Blaukat A (2003) The tyrosine kinase Pyk2 regulates Arf1 activity by phosphorylation and inhibition of the Arf-GTPase-activating protein ASAP1. *J Biol Chem* **278:** 29560–29570

Nauli SM, Alenghat FJ, Luo Y, Williams E, Vassilev P, Li X, Elia AE, Lu W, Brown EM, Quinn SJ, Ingber DE, Zhou J (2003) Polycystins 1 and 2 mediate mechanosensation in the primary cilium of kidney cells. *Nat Genet* **33:** 129–137

Otto E, Loeys B, Khanna H, Hellemans J, Sudbrak R, Fan S, Muerb U, O'Toole JF, Helou J, Attanasio M, Utsch B, Sayer JA, Lillo C, Jimeno D, Coucke P, de Paepe A, Reinhardt R, Klages S, Tsuda M, Kawakami I, Kusakabe T, Omran H, Imm A, Tippens M, Raymond PA, Hill J, Beales P, He S, Kispert A, Margolis B, Williams DS, Swaroop A, Hildebrandt F (2005) A novel ciliary IQ domain protein, NPHP5, is mutated in Senior–Loken syndrome (nephronophthisis with retinitis pigmentosa), and interacts with RPGR and calmodulin. *Nat Genet* **37:** 282–288

Otto EA, Schermer B, Obara T, O'Toole JF, Hiller KS, Mueller AM, Ruf RG, Hoefele J, Beekmann F, Landau D, Foreman JW, Goodship JA, Strachan T, Kispert A, Wolf MT, Gagnadoux MF, Nivet H, Antignac C, Walz G, Drummond IA, Benzing T, Hildebrandt F (2003) Mutations in INVS encoding inversin cause nephronophthisis type 2, linking renal cystic disease to the function of primary cilia and left–right axis determination. *Nat Genet* **34:** 413–420

Pan J, Wang Q, Snell WJ (2005) Cilium-generated signaling and cilia-related disorders. *Lab Invest* **85:** 452–463

Pazour GJ, Baker SA, Deane JA, Cole DG, Dickert BL, Rosenbaum JL, Witman GB, Besharse JC (2002) The intraflagellar transport protein, IFT88, is essential for vertebrate photoreceptor assembly and maintenance. *J Cell Biol* **157:** 103–113

Pazour GJ, Rosenbaum JL (2002) Intraflagellar transport and cilia-dependent diseases. *Trends Cell Biol* **12:** 551–555

Pazour GJ, Witman GB (2003) The vertebrate primary cilium is a sensory organelle. *Curr Opin Cell Biol* **15:** 105–110

Piguet V, Wan L, Borel C, Mangasarian A, Demaurex N, Thomas G, Trono D (2000) HIV-1 Nef protein binds to the cellular protein PACS-1 to downregulate class I major histocompatibility complexes. *Nat Cell Biol* **2:** 163–167

Praetorius HA, Spring KR (2001) Bending the MDCK cell primary cilium increases intracellular calcium. *J Membr Biol* **184:** 71–79

Rosenbaum JL, Witman GB (2002) Intraflagellar transport. *Nat Rev Mol Cell Biol* **3:** 813–825

Scott GK, Gu F, Crump CM, Thomas L, Wan L, Xiang Y, Thomas G (2003) The phosphorylation state of an autoregulatory domain controls PACS-1-directed protein traffic. *EMBO J* **22:** 6234–6244

Snell WJ, Pan J, Wang Q (2004) Cilia and flagella revealed: from flagellar assembly in *Chlamydomonas* to human obesity disorders. *Cell* **117:** 693–697

Tsiokas L, Kim E, Arnould T, Sukhatme VP, Walz G (1997) Homo- and heterodimeric interactions between the gene products of PKD1 and PKD2. *Proc Natl Acad Sci USA* **94:** 6965–6970

Wan L, Molloy SS, Thomas L, Liu G, Xiang Y, Rybak SL, Thomas G (1998) PACS-1 defines a novel gene family of cytosolic sorting proteins required for *trans*-Golgi network localization. *Cell* **94:** 205–216

Yoshino A, Bieler BM, Harper DC, Cowan DA, Sutterwala S, Gay DM, Cole NB, McCaffery JM, Marks MS (2003) A role for GRIP domain proteins and/or their ligands in structure and function of the *trans* Golgi network. *J Cell Sci* **116:** 4441–4454

